BBA - General Subjects 1862 (2018) 2104–2111

Contents lists available at ScienceDirect

BBA - General Subjects

journal homepage: www.elsevier.com/locate/bbagen

Stochastic simulations of nanoparticle internalization through transferrin receptor dependent clathrin-mediated endocytosis

Hua Deng, Prashanta Dutta, Jin Liu*

School of Mechanical and Materials Engineering, Washington State University, Pullman, WA 99164-2920, United States

ARTICLE INFO

Keywords:
Clathrin-coated pit
Drug delivery
Virus entry
Ligand-receptor interactions
Membrane deformation
Monte Carlo simulations

ABSTRACT

Background: Receptor dependent clathrin-mediated endocytosis (CME) is one of the most important endocytic pathways for the internalization of bioparticles into cells. During CME, the ligand-receptor interactions, development of clathrin-coated pit (CCP) and membrane evolution all act together to drive the internalization of bioparticles. In this work, we develop a stochastic computational model to investigate the CME based on the Metropolis Monte Carlo simulations.

Methods: The model is based on the combination of a stochastic particle binding model with a membrane model. The energetic costs of membrane bending, CCP formation and ligand-receptor interactions are systematically linked together.

Results: We implement our model to investigate the effects of particle size, ligand density and membrane stiffness on the overall process of CME from the drug delivery perspectives. Consistent with some experiments, our results show that the intermediate particle size and ligand density favor the particle internalization. Moreover, our results show that it is easier for a particle to enter a cell with softer membrane.

Conclusions: The model presented here is able to provide mechanistic insights into CME and can be readily modified to include other important factors, such as actins. The predictions from the model will aid in the therapeutic design of intracellular/transcellular drug delivery and antiviral interventions.

1. Introduction

Delivery of drugs utilizing nanoparticles has been of great interest in recent years. The drug containing particles can enter cells through passive diffusion [1–3], or through active interactions. Among them, the receptor-mediated endocytosis (RME) is one of the most important processes utilized by bioparticles (such as viruses [4–6] and drug carriers [7–9]) to enter the targeted cells. RME plays a central role in the control of essential cellular functions, modulation of membrane composition and regulation of many intracellular signaling cascades. Among the different types of endocytic pathways, the receptor dependent clathrin-mediated endocytosis (CME) is the most common pathway utilized by viruses. Therefore, CME is by far the most studied and well-characterized endocytic pathway. As shown in Fig. 1, CME is initiated by the interactions between ligands on the particle and the corresponding receptors on the cell membrane. The ligand-receptor binding triggers the transmembrane signals through, for example, the motifs of the cytoplasmic tails of receptors, which can be recognized by the endocytic components such as adapter complex 2 (AP2) and other accessory proteins [10]. Clathrin lattices are then recruited to the membrane inner leaflet at the endocytic site and form the clathrin-coated pit (CCP). The invagination of membrane, or budding, then takes place as a result of the accumulating effects from the curvature inducing proteins. After forming a mature vesicle, the clathrin-coated vesicle (CCV) finally pinches off from the cell membrane by the dynamins. Since CME can efficiently transport relatively large particles (~100 nm and bigger), it is critically important for the therapeutic design of antiviral interventions and intracellular/transcellular delivery of drug carriers [11].

CME of bioparticles is a complex process, that involves particle coating ligands and a variety of cellular proteins, such as receptors, and the multifactorial machineries and signaling pathways associated with the clathrin, dynamin, and microtubule networks to name a few [12–16]. During CME, the particles first bind to the plasma membrane through interactions between surface ligands and cell receptors, then enter the cell as a result of the collective and cooperative interplay of membrane alterations, multivalent interactions and other factors. This highly complex process is dynamic and dictated by a variety of physical and biochemical events, such as particle motions, membrane reshaping and remodeling, receptor diffusion and protein-protein, protein-lipid

* Corresponding author.
E-mail address: jin.liu2@wsu.edu (J. Liu).

https://doi.org/10.1016/j.bbagen.2018.06.018
Received 12 March 2018; Received in revised form 14 June 2018; Accepted 26 June 2018
Available online 28 June 2018
0304-4165/

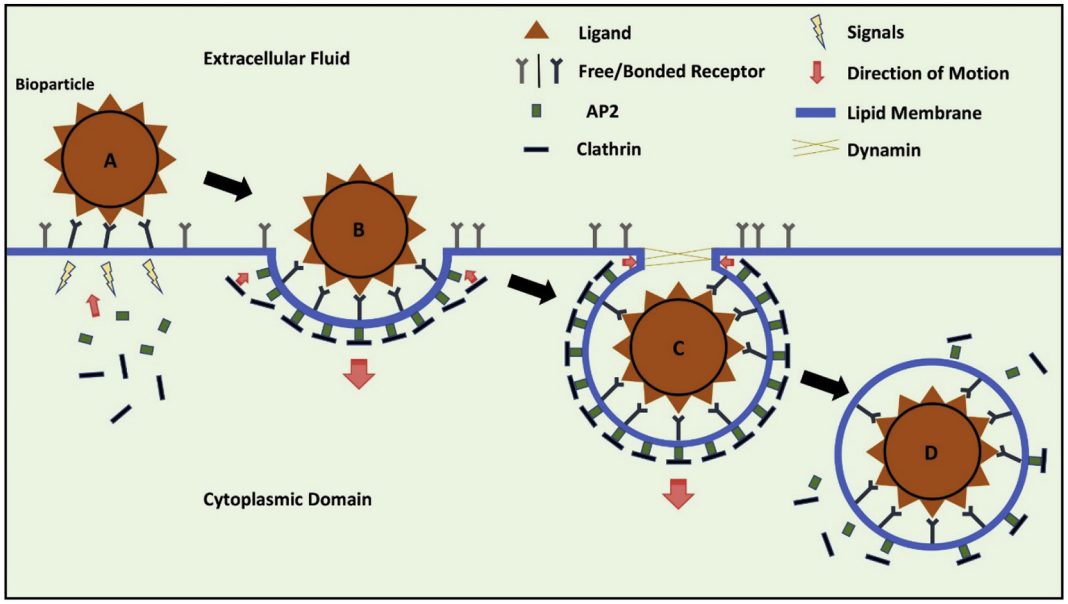

Fig. 1. Schematic of the receptor dependent clathrin-mediated endocytosis (CME). Particle first binds with membrane through ligand-receptor interactions, then ligand-receptor interactions trigger the assembly of clathrin and formation of clathrin-coated pits (CCP). CCPs cause the deformation of membrane and formation of clathrin-coated vesicle (CCP). Finally CCV pinches off from the membrane by dynamins.

interactions, occurring at multiple length and time scales.

Due to the complexity of the process, experimental exploration of CME is challenging. Theoretical continuum models have been developed to provide fundamental insights into CME of bioparticles [17–22]. In these models, the energetic and entropic contributions from molecular scale interactions are averaged and approximated by continuum functions and the total free energy functional of the system is formulated. On the other hand discrete models, such as coarse-grained molecular dynamics [23, 24] and dissipative particle dynamics [25–28], have also been used to study CME. Due to the high computational cost, the sizes of the particles considered in discrete models are relatively small.

In this work, we implement a stochastic computational model for bioparticle entry through CME with Metropolis Monte Carlo (MC) method, which allows us to study the extreme deformations like budding as well as the growing of clathrin lattices during the deformation. The model is an integration of a previously validated particle adhesion model with a powerful three-dimensional stochastic membrane model. We also introduce the impact of CCP through coupling the growth of CCP with the ligand-receptor interactions. By utilizing transferrin (Tf) and transferrin receptor (TfR) as the ligand and receptor, we investigate the effects of particle size, ligand density and membrane bending rigidity on the CME. Our results show that the internalization efficiency of the particle is dependent on the combined effects of the three parameters. There exits intermediate particle size and ligand density that maximize the probability of internalization which agree with experimental observations. Finally, we show that the endocytosis is more favorable for softer membranes.

2. Material and methods

2.1. Particle binding model

The interactions between the particle and membrane are through the specific interactions between the ligands on the particle and receptors on the cell surface, as indicated in Fig. 2. In our model, the particle is modeled as a rigid sphere and the particle surfaces is coated with a number of ligands that bind specifically to the receptors on the cell surface. The ligands and receptors are treated as cylinders with one end attached to the particle/membrane surface and the other free end as binding tip. The ligands are uniformly coated on the particle. The particle is allowed to translate and rotate. The receptors are placed normal to the local surface and can freely diffuse on the membrane. This model has been rigorously validated in our previous work [29–31].

2.2. Membrane deformation model

The topology and deformation of the cell membrane are modeled through Helfrich Hamiltonian [32], on a three-dimensional curvilinear triangulate system (see Fig. 3). The total energy E of the membrane is expressed as:

$$E = \iint \left[\frac{\kappa}{2}(2H - H_0)^2 + \overline{\kappa}K\right]dA \tag{1}$$

where κ and $\overline{\kappa}$ are the bending rigidity and Gaussian rigidity of the membrane. $H = (c_1 + c_2)/2$ is the mean curvature and $K = c_1c_2$, the Gaussian curvature of the surface, where c_1 and c_2 are the principal radii of curvatures. H_0 is the intrinsic or spontaneous mean curvature of the membrane. Since the membrane has fixed topological type in our simulation, the Gaussian term remains a constant and is hence not included in the model.

In this work, a square patch of cell membrane is discretized in a triangulate system. As illustrated in Fig. 3, the system consists of a number of vertices, links and triangles. Details regarding the membrane model can be found in Ref. [33]. Periodic boundary conditions are applied on the membrane boundaries.

2.3. Clathrin model

There is a long lasting debate on the driving force for the deformation of membrane and the role of clathrin during the vesicle budding [34–37]. In vitro, flat clathrin lattices can automatically form closed basket-like structure composed of pentagons and hexagons [38, 39]. This implies the closed basket-like structure is the energetically stable for clathrin assembly. Hinrichsen et al. [34] showed that clathrin is required for membrane budding. In the absence of clathrin, AP2 and other accessory proteins are able to form patches with similar size, but the patches do not have curvature. Recent work by Dannhauser and

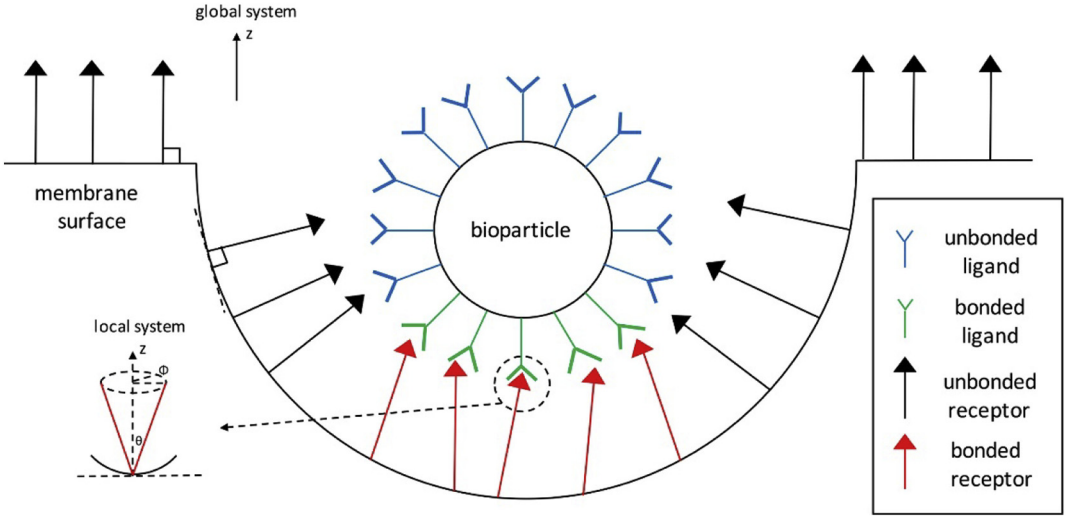

Fig. 2. Particle binding to membrane surface. The binding is through the interactions between ligands on the particle and receptors on the membrane surface. The bonded receptors (red) can bend and rotate, the free receptors (black) are always perpendicular to the local surface and can diffuse on the surface.

Ungewickell [37] has demonstrated that clathrin polymerization alone is able to provide sufficient curvature to bend the membrane and generate spherical buds.

In our clathrin model, the effects of clathrin on membrane are treated as additional intrinsic curvature and modified bending rigidity, and then the total energy of the system with clathrin is calculated as:

$$E = \iint \left[\frac{\kappa}{2}(2H)^2\right]dA + \iint \left[\frac{\kappa_{cla}}{2}(2H - H_{cla})^2\right]dA \quad (2)$$

The first term accounts for the regions without clathrin and the second term represents the effects from clathrin. κ_{cla} and H_{cla} are the bending rigidity and intrinsic curvature of the clathrin coat. Since the CCPs are attached to the membrane bilayer through accessory proteins, we assume the cell surface and clathrin patch share the same local mean curvature. Banerjee et al. [40] presented a similar one-dimensional model for clathrin assembly. In their model, two additional terms accounting for protein-protein and protein-lipid binding during the formation of CCP have been considered. In our model, we have neglected those detailed interactions.

The receptor molecules have specific signal sequences at the end of their cytoplasmic domain, which bind to the adaptor protein AP2 facilitating the recruitment of clathrin coats [41]. Experiments have shown that the binding affinity between AP2 and membrane is increased by about 25-fold in the presence of receptor proteins [42]. Binding to the corresponding ligand help stabilize the receptor molecules and may assist in AP2 recruitment leading to clathrin accumulation [43, 44]. Moreover, Ehrlich et al. [45] has demonstrated through experiment a steady growth of clathrin pit during the endocytosis of cargo (receptor) molecules. This indicates that the CCP is formed by the continuous accumulation of clathrin units. Based on the above evidences, the recruitment of the clathrin is modeled as a ligand-receptor dependent process. As shown in Fig. 3, each time when a new bond between ligand-receptor is formed, clathrin accumulates at the new binding site. The impact from clathrin is represented by the curvature field. An intrinsic curvature H_{cla} is applied to the vertices within an area, and the radius (14 nm) of the area is determined by the clathrin polygon detected from experiments [46]. In our simulations, $\kappa_{cla} = 200$ k_BT according to Ref. [40]. For H_{cla}, experiments showed that diameter of the clathrin vesicles ranges from 20 nm to 100 nm depending on the accessory proteins [47, 48]. Here we use $H_{cla} = 0.036$ nm^{-1} in

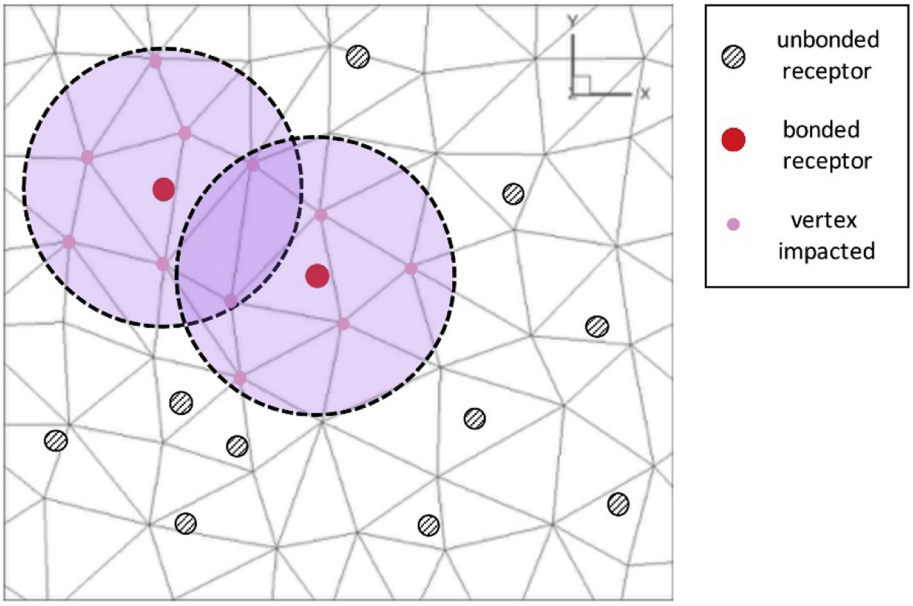

Fig. 3. Membrane and clathrin model. The membrane surface is discretized on a triangulate system consisting of vertices, links and triangles. For clathrin model, the newly bonded receptor (red dots) introduce the influence of clathrin lattices within a radius of 14 *nm*. The vertices within the area are impacted by the intrinsic curvature of clathrin lattices. Unbonded receptors do not affect the distribution of clathrin.

simulations. The local clathrin will disappear if the nanoparticle completely detaches from the membrane surface.

2.4. Coupling of particle binding with membrane deformation

Once the bioparticle approaches the membrane surface, biochemical reactions between ligand and receptor may take place. The ligand-receptor interactions are modeled through the Bell model [49]:

$$\Delta G_r(d) = \Delta G_0 + \frac{1}{2}kd^2 \tag{3}$$

where d is the distance between the binding tips of the interacting ligand-receptor, ΔG_0 is the equilibrium free energy change at $d = 0$, and k is the interaction bond force constant. The flexural movement of the receptors is another crucial component for antibody-receptor interactions since it is directly related to the entropy change during binding. For the receptor flexural movement, we allow the receptors to bend and rotate relative to the local normal direction. Under the assumption of small flexural deformations, we can model the flexure of a receptor as bending a beam from equilibrium (normal to cell surface) position, and the bending energy due to flexure can be calculated as:

$$\Delta G_f(\theta) = (2EI/L)\theta^2 \tag{4}$$

where EI is the receptor flexural rigidity, L is the receptor length and θ represents the bending angle from the normal axis of the local triangle. The flexural rigidity is set to the rigidities between glycoproteins and actin filament [50]. The geometric parameters (such as the size of the ligands, receptors) are obtained from the crystal structures of the corresponding protein, and the reaction parameters (such as ΔG_0, k, and reactive compliance) are determined by fitting the experimental data. Details on the determination of the parameters can be found in previous work [29]. The binding energy change for each interaction is the difference between the energy reduction by ligand-receptor interaction and the energy increase through receptor bending.

Our system contains the following Monte Carlo steps: receptor diffusion, particle translation or rotation and membrane surface evolution. During receptor diffusion and particle translation/rotation, the membrane topology is fixed. For free receptors, they always move on the membrane surface and the receptors are pointed to the normal direction of the local surface. For the bonded receptors, new tip position is calculated through Rodrigues's rotation formula, which is able to transform the coordinates between two different Cartesian systems while keep the length and bending angle of the receptor unchanged. When the particle is translated or rotated, the ligands are translated or rotated along with the particle. The particle translation/rotation may cause the reaction energy change or even breakage of bonds between ligands and receptors. If the distance between the tips of the bonded antibody and receptor is greater than the reaction range after the movement, then this bond breaks and the receptor tip position is reset to be perpendicular to its local triangle.

On the other hand, during the membrane surface evolution, the positions of the particle and ligands are kept fixed. The membrane evolution causes the rearrangement of corresponding triangles. If a receptor belongs to any of the affected triangles, the position of the receptor should be adjusted accordingly. If the membrane movement causes the position change of any bonded receptor, then the variation of binding energy of the receptor should also be considered when calculating the total free energy change.

In each Monte Carlo step, one of the movements from above will be randomly selected and the system energy (U) for the new configuration (U_{new} contains contributions from membrane elastic energy E (Eq. (2)), ligand-receptor reaction energy ΔG_r (Eq. (3)) and the receptor flexural energy ΔG_f (Eq. (4))) will be calculated, and then the new configuration will be accepted with the following probability: $\min\{1, \exp[-(U_{\text{new}} - U_{\text{old}})/k_BT]\}$, where k_B is the Boltzmann constant and T is the system temperature. In addition, we will also account for the ligand-receptor bond formation and breakage by a stochastic process. Within a reaction distance, a ligand-receptor pair will be randomly selected and if they are unbonded, the bond will form according to the following probability: $\min\{1, \exp[-\Delta G/k_BT]\}$. If the pair is already bonded, the bond will break according to $\min\{1, \exp[\Delta G/k_BT]\}$, where ΔG is the energy change due to the bond formation/breakage calculated from Eqs. (3) and (4). It is worth to mention that, different from the physical time steps in regular molecular simulations, our Monte Carlo simulations are seeking equilibrium configurations of the system by sampling different energy states generated at different Monte Carlo steps.

3. Results and discussion

Receptor dependent CME has been the most studied and well-characterized pathway for targeted drug delivery [51, 52]. Among various targeting receptors, the cellular transferrin receptors (TfRs) have been identified as promising targets for many diseases. TfRs play crucial roles during cellular iron transport for various types of cells [53–56], therefore the TfRs are usually overexpressed in malignant cells which need high level of irons for cell growth [57]. As a result, the corresponding ligand, transferrin (Tf), has been actively used for various drug delivery designs [7, 58, 59]. For example, the Tf conjugated anticancer nanoparticles have been found to increase the uptake against tumor cells with overexpressed TfRs [60–62]. Moreover, Tf coated nanoparticles have been designed for effective delivery of drugs across blood-brain barrier (BBB) [63, 64]. In this work, we implement our model to investigate the TfR-dependent CME process for drug delivery. Thus, the parameters for ligand-receptor interactions are chosen to mimic Tf-TfR binding. A summary of the simulation parameters is provided in Table 1. In the following sections, a number of important design parameters, such as the particle size, ligand density and membrane bending rigidity, will be studied in details.

3.1. Effect of particle size

The size of clathrin-coated pits (CCP) during the CME varies for different species and cell types. The yeasts and plants such as Saccharomyces cerevisiae and Arabidopsis have small vesicle size of ~ 30–60 nm in diameter, while vesicles with diameter ~200 nm in mammalian cells such as chicken oocytes are observed [72, 73]. In virus entry, an average diameter of at least ~120 nm vesicle is required for a spherical influenza virus [74]. Large vesicles with at least 180 nm in diameter are needed for the vesicular stomatitis virus (VSV) [75]. The size of the vesicles depends largely on the size of the cargos [15]. Rejman et al. [76] have shown in cell culture experiments that the particle size strongly affected the cellular uptake efficiency, and even the endocytic pathways. They demonstrated that smaller particles

Table 1
Summary of parameters used in the simulations.

Parameters	Value	Ref
Size of membrane surface	910 nm × 910 nm	
Membrane bending rigidity κ_m	20 to 100 k_BT	[65]
Clathrin bending rigidity κ_{cla}	200 k_BT	[66]
Clathrin intrinsic curvature H_{cla}	0.036 nm^{-1}	[47]
Nanocarrier diameter	40 to 160 nm	
Transferrin receptor length	9.3 nm	[67]
Transferrin receptor radius	5 nm	[67]
Transferrin length	9 nm	[68]
Transferrin radius	2.5 nm	[68]
Number of transferrin receptors	300	[69]
Number of transferrins per particle	20 to 418	[70]
Equilibrium free energy change ΔG_0	$-8.64e^{-20}$ J	[71]
Reactive compliance (reaction cutoff)	0.9 nm	[71]
Receptor flexural rigidity EI	7000 pN·nm^2	[50]
System temperature	298 K	

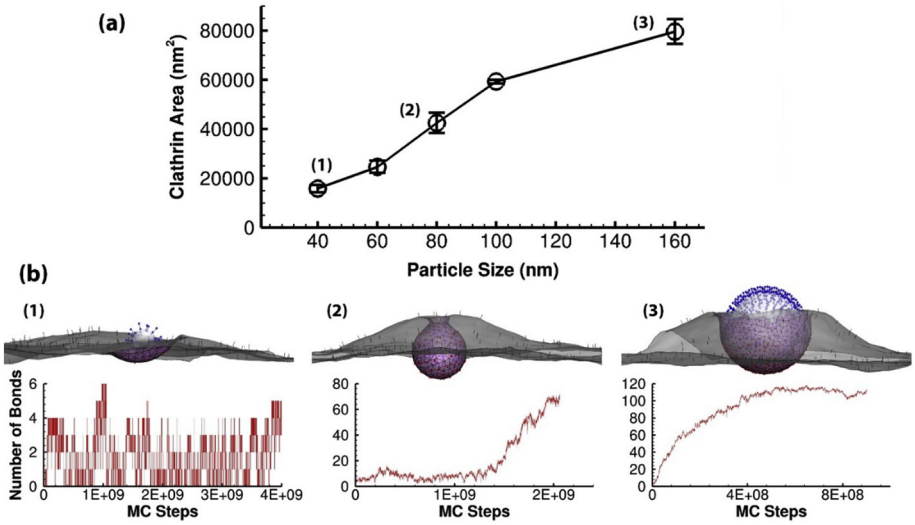

Fig. 4. Effect of particle size: (a) Area of CCP at different particle sizes. The standard deviation is based on 5 independent simulations. (b) The equilibrium profiles of the membrane-particle systems with particle diameters of 40, 80 and 160 *nm*, and the corresponding number of Tf-TfR bonds formed during MC simulations. The CCP (pink), bonded TfR (red), free TfR (black), bonded Tf (green) and unbonded Tf (blue) are all shown in the profiles.

(< 200 nm in diameter) enter cell through clathrin-mediated endocytosis, while larger particles (500 nm in diameter) through caveolae-mediated endocytosis. Moreover, recent experiments [70] have shown that the size of the particles played important roles during receptor-mediated transcytosis of nanoparticle across blood-brain barrier. Hence, the particle size is a key design factor for biomedical applications. Many studies have demonstrated the importance of particle size and also found that there exits an optimal particle size with higher efficiency than either smaller or larger particle sizes [77–79].

We study the particle size effect on clathrin recruitment and endocytosis by varying the particle sizes from 40 to 160 nm in diameters. We assumed a constant ligand density of ~ 5200/μm^2, which is lower than the maximum Tf content density on a spherical particle [70]. The membrane surface has a bending rigidity of 20 k_BT in all cases.

Fig. 4(a) shows the area of CCP as a function of different particle sizes. In general, larger particles cause the formation of larger CCP. Fig. 4(b) shows the equilibrium profiles of the membrane-particle systems with small (40 nm), medium (80 nm) and large (160 nm) particles, and the corresponding number of ligand-receptor bonds as a function of Monte Carlo steps. As shown, for small particles, small area of CCP (pink area) is formed as the particle approaches to the membrane and Tf-TfR interactions take place. However, no clear invagination of membrane is observed throughout the simulations and the particle frequently attaches to and detaches from the membrane surface. As indicated from the bond formation, only a few bonds form and break and the number of bonds often goes to zero throughout the simulations. This is consistent with the experimental observations that certain threshold clustering of small particles has to be reached to trigger the internalization process [80]. As the particle size is increased, more Tf-TfR bonds are formed stimulating the accumulation of CCP. As a results, the membrane rapidly wraps the particle and a mature vesicle with clear neck region is observed. On the other hand, when the particle size is further increased, as shown in Fig. 4(b), the particle internalization becomes more difficult. Internalization of larger particles requires larger CCPs, but depletion of the local receptors affects the clathrin accumulation and delays the internalization. As illustrated in the bond formation, the number of Tf-TfR bonds quickly increases at the beginning of the attachment and then saturates. This effect is reflected as the nonlinear behavior at larger particle size in Fig. 4(a).

3.2. Ligand density effect

The ligand density on the particle is another tunable parameter influencing the CME during drug delivery. Banerjee et al. [81] has shown that the cellular uptake through CME was proportional to the ligand density of Tf conjugated particles. In a recent mice study, Wiley et al. [70] has demonstrated that the Tf coated gold nanoparticles can be transported from the luminal side of the BBB to the brain parenchyma. They found that gold nanoparticles with high density of transferrin remain strongly attached to brain ECs, whereas nanoparticles with relatively low transferrin density can pass through the EC and released in the brain side. However, nanoparticles did not attach to receptors on the BBB if the transferrin density is too low. To investigate the ligand density effect on the CME, we fix the particle size at 100 *nm* and vary the number of ligands on particle as 20, 30, 40, 60, 100, 162 and 200. These correspond to ligand densities from 645 to 6500/μm^2.

As shown in Fig. 5(a), the area of CCP increases rapidly with the ligand density initially, but saturates after ligand density of 1935/μm^2. At low ligand density (970/μm^2), as indicated in Fig. 5(b), only a few Tf-TfR bonds form and break, triggering the appearance and disappearance of small areas of CCP. The interaction between particle and membrane is also weak and the particle is moving around on the membrane. At high ligand density (1935/μm^2), on the other hand, the particle firmly attaches to the cell surface as a result of increased number of Tf-TfR bonds. Simultaneously the area of CCP increases and eventually a clear vesicle is observed. Further increasing the ligand density will cause an increase of the number of ligand-receptor bonds but not affect the area of CCP. However, the increased number of bonds may cause a depletion of available receptors and slow down internalization of surrounding particles. It is interesting to find that the result for intermediate ligand density (1290/μm^2) is rather scattered as indicated by the standard deviation. At this ligand density, 3 out of 5 independent simulations show dynamic binding as illustrated in Fig. 5(b) and 2 simulations show completely internalization (see Fig. 6 below).

3.3. Membrane rigidity effect

The CME depends not only on the particle but also on the mechanical properties of cell membrane. The membrane bending rigidity represents the stiffness of the plasma surface. Different types of cells have different membrane bending rigidities depending on membrane compositions, cell cytoskeleton and temperatures. Besides, diseases or viruses such as cancer and HIV infection may cause stiffness change compared with their healthy counterparts, which demonstrates the importance of membrane bending rigidity in drug design [82–84]. To evaluate the role of membrane rigidity on CME, we fix the particle size and ligand density at 100 nm and 5225/μm^2 respectively, and vary the membrane bending rigidities at 20, 40, 60, 80 and 100 k_BT [65, 85].

The membrane stiffness affects the membrane's ability to

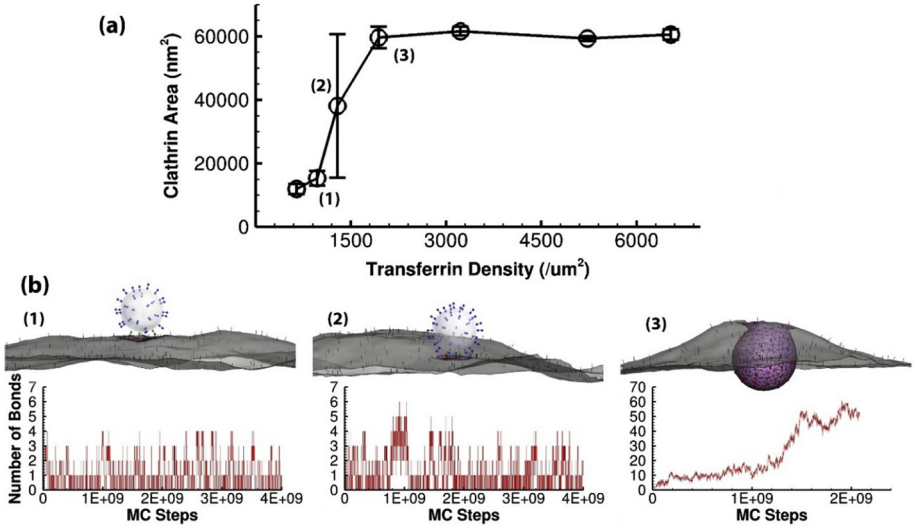

Fig. 5. Effect of ligand density: (a) Area of CCP at different ligand densities. The standard deviation is based on 5 independent simulations. (b) The equilibrium profiles of the membrane-particle systems with ρ_{ab} = 970, 1290 and 1935/μm^2 and the corresponding number of Tf-TfR bonds formed during MC simulations. The CCP (pink), bonded TfR (red), free TfR (black), bonded Tf (green) and unbonded Tf (blue) are all shown in the profiles.

accommodate endocytic deformation caused by clathrin. As shown in Fig. 7(a), the area of CCP is decreased with the membrane bending rigidities. The dependence of CME on bending rigidity is through the competition among the ligand-receptor binding, clathrin accumulation and membrane deformation. It is easier for a soft membrane to deform and form the vesicle, while stiffer membrane has more resistant to the deformation. Upon ligand-receptor interaction, the clathrin coat is recruited to the membrane surface and causes local deformation. Soft membrane is able to accommodate the deformation and triggers the formation of more ligand-receptor bonds. As illustrated in Fig. 7(b), increasing the membrane bending rigidity significantly reduces the number of bonds and area of CCP. Our results indicate that the internalization of particles is easier for softer membranes.

4. Conclusions

The clathrin-mediated endocytosis (CME) is a complicated endocytic mechanism involving molecular scale level ligand-receptor interaction as well as cellular level particle and membrane movement. In this paper, we developed a stochastic model based on Monte Carlo simulations for the process of CME. The model is capable of capturing the extreme membrane deformation as well as the growth of the clathrin-coated pits. We implemented our model to study the internalization of transferrin coated nanoparticles through transferrin-receptor dependent CME, and systematically investigated the effects from particle size, ligand density and membrane bending rigidity.

Our results showed that the particle size played an important role in the CME. For a single particle, there exists a critical size below which the particle cannot trigger the internalization. Consistent with experiments [80], clustering of particles is required for CME. Internalization of much larger particles may also become difficult due to the depletion of the local receptors. Therefore, a size of 80–100 nm is better for CME according to our simulations. The ligand density on particles also significantly impact CME. A threshold ligand density must be overcome to achieve internalization. Excessive ligand coverage may cause unnecessary ligand-receptor bonds, and reduce the free receptors leading to adverse effect on internalization. Growing number of experiments showed that the cancer cells are softer than normal cells [84]. Our study of membrane bending rigidity effect indicated that the internalization of particles through CME is easier for softer membranes.

Finally, a number of assumptions have been made to simplify our model. Considering the complexity in biological environment and uncertainties in experimental conditions, our comparisons with experiments can only be qualitative. For example, it has been shown that the transferrin coated nanoparticles lose their targeting ability when they are place in certain biological environment [86]. Other important assumptions in our model include a uniform ligand distribution on particles and a simple spring model for ligand-receptor interactions, which are far more idealized compared with realistic experiments. Nevertheless, our model is able to provide valuable mechanistic insights on this complex process. With the development of quantitative characterization techniques [87, 88], and refinement of our model, we expect that more quantitative comparisons between model and experiments are possible.

Acknowledgments

Research reported in this publication was supported by the National Institute of General Medical Sciences of the National Institutes of Health under Award Number R01GM122081. The content is solely the responsibility of the authors and does not necessarily represent the official views of the National Institutes of Health. Computational resources were provided in part by the Extreme Science and Engineering Discovery Environment (XSEDE) under grant No. MCB170012.

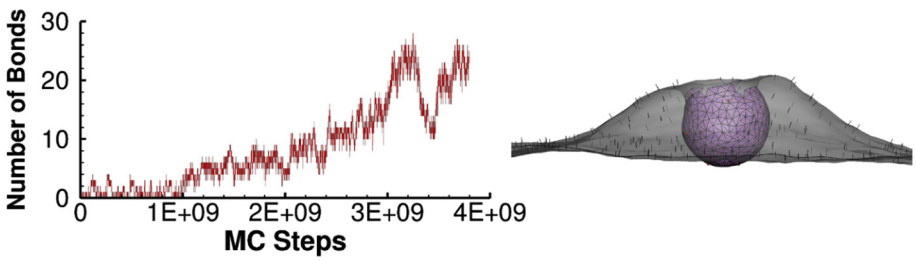

Fig. 6. The number of Tf-TfR bonds as a function of MC steps (left) and the profile of the membrane particle system (right) for the case with ligand density of 1290/μm^2 and with vesicle formation.

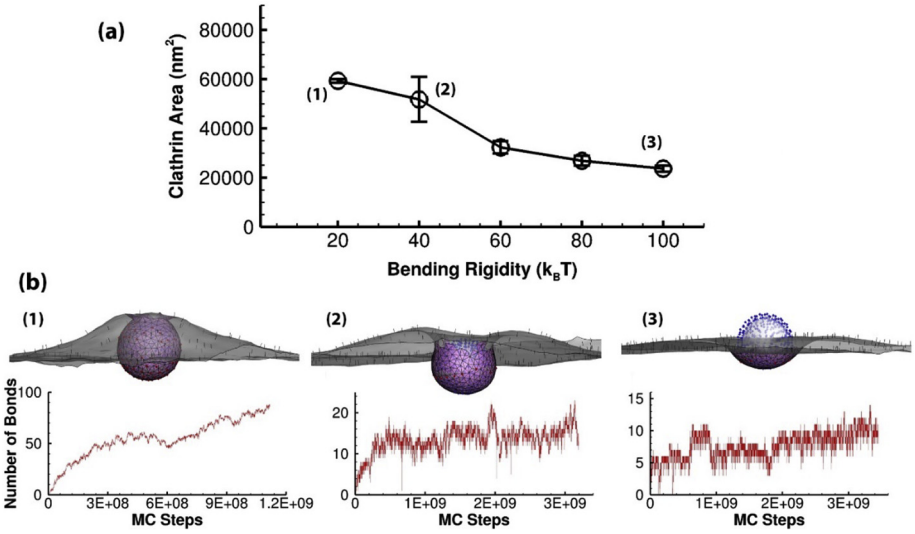

Fig. 7. Effect of membrane bending rigidity: (a) Area of CCP at different membrane bending rigidities. The standard deviation is based on 5 independent simulations. (b) The equilibrium profiles of the membrane-particle systems with membrane bending rigidities of 20, 40 and 100 k_BT. The CCP (pink), bonded TfR (red), free TfR (black), bonded Tf (green) and unbonded Tf (blue) are all shown in the profiles.

References

[1] R. Sijbesma, G. Srdanov, F. Wudl, J.A. Castoro, C. Wilkins, S.H. Friedman, D.L. Decamp, G.L. Kenyon, Synthesis of a fullerene derivative for the inhibition of HIV enzymes, J. Am. Chem. Soc. 115 (1993) 6510–6512.
[2] J.M. Ashcroft, D.A. Tsyboulski, K.B. Hartman, T.Y. Zakharian, J.W. Marks, R.B. Weisman, M.G. Rosenblum, L.J. Wilson, Fullerene (C-60) immunoconjugates: interaction of water-soluble C-60 derivatives with the murine anti-gp240 melanoma antibody, Chem. Commun. (2006) 3004–3006.
[3] R. Qiao, A.P. Roberts, A.S. Mount, S.J. Klaine, P.C. Ke, Translocation of C-60 and its derivatives across a lipid bilayer, Nano Lett. 7 (2007) 614–619.
[4] M. Marsh, A. Helenius, Virus entry: open sesame, Cell 124 (2006) 729–740.
[5] J. Mercer, M. Schelhaas, A. Helenius, Virus entry by endocytosis, Annu. Rev. Biochem. 79 (2010) 803–833.
[6] J. Grove, M. Marsh, The cell biology of receptor-mediated virus entry, J. Cell Biol. 195 (2011) 1071–1082.
[7] D. Peer, J.M. Karp, S. Hong, O.C. Farokhzad, R. Margalit, R. Langer, Nanocarriers as an emerging platform for cancer therapy, Nat. Nanotechnol. 2 (2007) 751–760.
[8] D.K. Bonner, C. Leung, J. Chen-Liang, L. Chingozha, R. Langer, P.T. Hammond, Intracellular trafficking of polyamidoamine–poly(ethylene glycol) block copolymers in DNA delivery, Bioconjug. Chem. 22 (2011) 1519–1525.
[9] J. Han, B.J. Zern, V.V. Shuvaev, P.F. Davies, S. Muro, V. Muzykantov, Acute and chronic shear stress differently regulate endothelial internalization of nanocarriers targeted to platelet-endothelial cell adhesion molecule-1, ACS Nano 6 (2012) 8824–8836.
[10] L.M. Traub, J.S. Bonifacino, Cargo recognition in clathrin-mediated endocytosis, Cold Spring Harb. Perspect. Biol. 5 (2013) a016790.
[11] I. Canton, G. Battaglia, Endocytosis at the nanoscale, Chem. Soc. Rev. 41 (2012) 2718–2739.
[12] L. Pelkmans, E. Fava, H. Grabner, M. Hannus, B. Habermann, E. Krausz, M. Zerial, Genome-wide analysis of human kinases in clathrin- and caveolae/raft-mediated endocytosis, Nature 436 (2005) 78–86.
[13] M. Kaksonen, C.P. Toret, D.G. Drubin, A modular design for the clathrin- and actin-mediated endocytosis machinery, Cell 123 (2005) 305–320.
[14] G.J. Doherty, H.T. McMahon, Mechanisms of endocytosis, Annu. Rev. Biochem. 78 (2009) 857–902.
[15] H.T. McMahon, E. Boucrot, Molecular mechanism and physiological functions of clathrin-mediated endocytosis, Nat. Rev. Mol. Cell Biol. 12 (2011) 517–533.
[16] W. Kukulski, M. Schorb, M. Kaksonen, John A.G. Briggs, Plasma membrane reshaping during endocytosis is revealed by time-resolved Electron tomography, Cell 150 (2012) 508–520.
[17] H.J. Gao, W.D. Shi, L.B. Freund, Mechanics of receptor-mediated endocytosis, Proc. Natl. Acad. Sci. U. S. A. 102 (2005) 9469–9474.
[18] S.X. Sun, D. Wirtz, Mechanics of enveloped virus entry into host cells, Biophys. J. 90 (2006) L10–L12.
[19] P. Decuzzi, M. Ferrari, The role of specific and non-specific interactions in receptor-mediated endocytosis of nanoparticles, Biomaterials 28 (2007) 2915–2922.
[20] P. Decuzzi, M. Ferrari, The receptor-mediated endocytosis of nonspherical particles, Biophys. J. 94 (2008) 3790–3797.
[21] S. Zhang, J. Li, G. Lykotrafitis, G. Bao, S. Suresh, Size-dependent endocytosis of nanoparticles, Adv. Mater. 21 (2009) 419–424.
[22] D. Gonzalez-Rodriguez, A.I. Barakat, Dynamics of receptor-mediated nanoparticle internalization into endothelial cells, PLoS One 10 (2015).
[23] R. Vacha, F.J. Martinez-Veracoechea, D. Frenkel, Receptor-mediated endocytosis of nanoparticles of various shapes, Nano Lett. 11 (2011) 5391–5395.
[24] X. Shi, A. von Dem Bussche, R.H. Hurt, A.B. Kane, H. Gao, Cell entry of one-dimensional nanomaterials occurs by tip recognition and rotation, Nat. Nanotechnol. 6 (2011) 714–719.
[25] T. Yue, X. Zhang, Molecular understanding of receptor-mediated membrane responses to ligand-coated nanoparticles, Soft Matter 7 (2011) 9104–9112.
[26] Y. Li, T. Yue, K. Yang, X. Zhang, Molecular modeling of the relationship between nanoparticle shape anisotropy and endocytosis kinetics, Biomaterials 33 (2012) 4965–4973.
[27] H.-m. Ding, Y.-q. Ma, Role of physicochemical properties of coating ligands in receptor-mediated endocytosis of nanoparticles, Biomaterials 33 (2012) 5798–5802.
[28] T. Yue, X. Zhang, Molecular modeling of the pathways of vesicle-membrane interaction, Soft Matter 9 (2013) 559–569.
[29] J. Liu, G.E.R. Weller, B. Zern, P.S. Ayyaswamy, D.M. Eckmann, V.R. Muzykantov, R. Radhakrishnan, Computational model for nanocarrier binding to endothelium validated using in vivo, in vitro, and atomic force microscopy experiments, Proc. Natl. Acad. Sci. U. S. A. 107 (2010) 16530–16535.
[30] J. Liu, R. Bradley, D.M. Eckmann, P.S. Ayyaswamy, R. Radhakrishnan, Multiscale modeling of functionalized nanocarriers in targeted drug delivery, Curr. Nanosci. 7 (2011) 727–735.
[31] J. Liu, N.J. Agrawal, A. Calderon, P.S. Ayyaswamy, D.M. Eckmann, R. Radhakrishnan, Multivalent binding of nanocarrier to endothelial cells under shear flow, Biophys. J. 101 (2011) 319–326.
[32] W. Helfrich, Elastic properties of lipid bilayers: theory and possible experiments, Z. Naturforsch. C 28 (1973) 693–703.
[33] N. Ramakrishnan, P.B.S. Kumar, J.H. Ipsen, Monte Carlo simulations of fluid vesicles with in-plane orientational ordering, Phys. Rev. E 81 (2010) 041922.
[34] L. Hinrichsen, A. Meyerhoiz, S. Groos, E.J. Ungewickell, Bending a membrane: how clathrin affects budding, Proc. Natl. Acad. Sci. U. S. A. 103 (2006) 8715–8720.
[35] S.J. Royle, The cellular functions of clathrin, Cell. Mol. Life Sci. 63 (2006) 1823–1832.
[36] R. Nossal, Energetics of clathrin basket assembly, Traffic 2 (2001) 138–147.
[37] P.N. Dannhauser, E.J. Ungewickell, Reconstitution of clathrin-coated bud and vesicle formation with minimal components, Nat. Cell Biol. 14 (2012) 634–639.
[38] J.H. Hurley, E. Boura, L.A. Carlson, B. Rozycki, Membrane budding, Cell 143 (2010) 875–887.
[39] A. Fotin, Y.F. Cheng, P. Sliz, N. Grigorieff, S.C. Harrison, T. Kirchhausen, T. Walz, Molecular model for a complete clathrin lattice from electron cryomicroscopy, Nature 432 (2004) 573–579.
[40] A. Banerjee, A. Berezhkovskii, R. Nossal, Stochastic model of Clathrin-coated pit assembly, Biophys. J. 102 (2012) 2725–2730.
[41] J.S. Bonifacino, L.M. Traub, Signals for sorting of transmembrane proteins to endosomes and lysosomes, Annu. Rev. Biochem. 72 (2003) 395–447.
[42] D. Ricotta, S.D. Conner, S.L. Schmid, K. von Figura, S. Honing, Phosphorylation of the AP2 m subunit by AAK1 mediates high affinity binding to membrane protein sorting signals, J. Cell Biol. 156 (2002) 791–795.
[43] J. Schlessinger, Cell signaling by receptor tyrosine kinases, Cell 103 (2000) 211–225.
[44] J.X. Chen, J.Z. Wang, K.R. Meyers, C.A. Enns, Transferrin-directed internalization and cycling of transferrin receptor 2, Traffic 10 (2009) 1488–1501.
[45] M. Ehrlich, W. Boll, A. van Oijen, R. Hariharan, K. Chandran, M.L. Nibert, T. Kirchhausen, Endocytosis by random initiation and stabilization of clathrin-coated pits, Cell 118 (2004) 591–605.
[46] J. Heuser, T. Kirchhausen, Deep-etch views of clathrin assemblies, J. Ultrastruct. Res. 92 (1985) 1–27.
[47] S. Zaremba, J.H. Keen, Assembly polypeptides from coated vesicles mediate reassembly of unique clathrin coats, J. Cell Biol. 97 (1983) 1339–1347.
[48] M.G.J. Ford, I.G. Mills, B.J. Peter, Y. Vallis, G.J.K. Praefcke, P.R. Evans, H.T. McMahon, Curvature of clathrin-coated pits driven by epsin, Nature 419 (2002) 361–366.
[49] G.I. Bell, M. Dembo, P. Bongrand, Competition between nonspecific repulsion and specific bonding, Biophys. J. 45 (1984) 1051–1064.

[50] S. Weinbaum, X.B. Zhang, Y.F. Han, H. Vink, S.C. Cowin, Mechanotransduction and flow across the endothelial glycocalyx, Proc. Natl. Acad. Sci. U. S. A. 100 (2003) 7988–7995.
[51] L.A. Bareford, P.W. Swaan, Endocytic mechanisms for targeted drug delivery, Adv. Drug Deliv. Rev. 59 (2007) 748–758.
[52] H. Hillaireau, P. Couvreur, Nanocarriers' entry into the cell: relevance to drug delivery, Cell. Mol. Life Sci. 66 (2009) 2873–2896.
[53] J.H. Jandl, J.K. Inman, R.L. Simmons, D.W. Allen, Transfer of iron from serum iron-binding protein to human reticulocytes, J. Clin. Invest. 38 (1959) 161–185.
[54] T.A. Hamilton, H.G. Wada, H.H. Sussman, Identification of transferrin receptors on the surface of human cultured cells, Proc. Natl. Acad. Sci. 76 (1979) 6406–6410.
[55] W.A. Jefferies, M.R. Brandon, S.V. Hunt, A.F. Williams, K.C. Gatter, D.Y. Mason, Transferrin receptor on endothelium of brain capillaries, Nature 312 (1984) 162–163.
[56] A.I. Khan, J. Liu, P. Dutta, Iron transport kinetics through blood-brain barrier endothelial cells, BBA Gen. Subj. 1862 (2018) 1168–1179.
[57] H.Y. Li, Z.M. Qian, Transferrin/transferrin receptor-mediated drug delivery, Med. Res. Rev. 22 (2002) 225–250.
[58] Z.M. Qian, H.Y. Li, H.Z. Sun, K. Ho, Targeted drug delivery via the transferrin receptor-mediated endocytosis pathway, Pharmacol. Rev. 54 (2002) 561–587.
[59] H.Y. Li, H.Z. Sun, Z.M. Qian, The role of the transferrin-transferrin-receptor system in drug delivery and targeting, Trends Pharmacol. Sci. 23 (2002) 206–209.
[60] D.A. Eavarone, X.J. Yu, R.V. Bellamkonda, Targeted drug delivery to C6 glioma by transferrin-coupled liposomes, J. Biomed. Mater. Res. 51 (2000) 10–14.
[61] C. Dufes, J.M. Muller, W. Couet, J.C. Olivier, I.F. Uchegbu, A.G. Schatzlein, Anticancer drug delivery with transferrin targeted polymeric chitosan vesicles, Pharm. Res. 21 (2004) 101–107.
[62] S.K. Sahoo, V. Labhasetwar, Enhanced antiproliferative activity of transferrin-conjugated paclitaxel-loaded nanoparticles is mediated via sustained intracellular drug retention, Mol. Pharm. 2 (2005) 373–383.
[63] V. Mishra, S. Mahor, A. Rawat, P.N. Gupta, P. Dubey, K. Khatri, S.P. Vyas, Targeted brain delivery of AZT via transferrin anchored pegylated albumin nanoparticles, J. Drug Target. 14 (2006) 45–53.
[64] K. Ulbrich, T. Hekmatara, E. Herbert, J. Kreuter, Transferrin- and transferrin-receptor-antibody-modified nanoparticles enable drug delivery across the blood-brain barrier (BBB), Eur. J. Pharm. Biopharm. 71 (2009) 251–256.
[65] E. Evans, W. Rawicz, Entropy-driven tension and bending elasticity in condensed-fluid membranes, Phys. Rev. Lett. 64 (1990) 2094–2097.
[66] A.J. Jin, K. Prasad, P.D. Smith, E.M. Lafer, R. Nossal, Measuring the elasticity of clathrin-coated vesicles via atomic force microscopy, Biophys. J. 90 (2006) 3333–3344.
[67] H. Fuchs, U. Lucken, R. Tauber, A. Engel, R. Gessner, Structural model of phospholipid-reconstituted human transferrin receptor derived by electron microscopy, Structure 6 (1998) 1235–1243.
[68] H.M. Berman, J. Westbrook, Z. Feng, G. Gilliland, T.N. Bhat, H. Weissig, I.N. Shindyalov, P.E. Bourne, The Protein Data Bank, Nucleic Acids Res. 28 (2000) 235–242.
[69] J.D. Bleil, M.S. Bretscher, Transferrin receptor and its recycling in hela-cells, EMBO J. 1 (1982) 351–355.
[70] D.T. Wiley, P. Webster, A. Gale, M.E. Davis, Transcytosis and brain uptake of transferrin-containing nanoparticles by tuning avidity to transferrin receptor, Proc. Natl. Acad. Sci. U. S. A. 110 (2013) 8662–8667.
[71] A. Yersin, T. Osada, A. Ikai, Exploring transferrin-receptor interactions at the single-molecule level, Biophys. J. 94 (2008) 230–240.
[72] I.I. Smaczynska-De Rooij, E.G. Allwood, S. Aghamohammadzadeh, E.H. Hettema, M.W. Goldberg, K.R. Ayscough, A role for the dynamin-like protein Vps1 during endocytosis in yeast, J. Cell Sci. 123 (2010) 3496–3506.
[73] P. Dhonukshe, F. Aniento, I. Hwang, D.G. Robinson, J. Mravec, Y.D. Stierhof, J. Friml, Clathrin-mediated constitutive endocytosis of PIN auxin efflux carriers in Arabidopsis, Curr. Biol. 17 (2007) 520–527.
[74] A. Harris, G. Cardone, D.C. Winkler, J.B. Heymann, M. Brecher, J.M. White, A.C. Steven, Influenza virus pleiomorphy characterized by cryoelectron tomography, Proc. Natl. Acad. Sci. U. S. A. 103 (2006) 19123–19127.
[75] D.K. Cureton, R.H. Massol, S. Saffarian, T.L. Kirchhausen, S.P.J. Whelan, Vesicular stomatitis virus enters cells through vesicles incompletely coated with Clathrin that depend upon actin for internalization, PLoS Pathog. 5 (2009).
[76] J. Rejman, V. Oberle, I.S. Zuhorn, D. Hoekstra, Size-dependent internalization of particles via the pathways of clathrin-and caveolae-mediated endocytosis, Biochem. J. 377 (2004) 159–169.
[77] F. Osaki, T. Kanamori, S. Sando, T. Sera, Y. Aoyama, A quantum dot conjugated sugar ball and its cellular uptake on the size effects of endocytosis in the subviral region, J. Am. Chem. Soc. 126 (2004) 6520–6521.
[78] B.D. Chithrani, A.A. Ghazani, W.C.W. Chan, Determining the size and shape dependence of gold nanoparticle uptake into mammalian cells, Nano Lett. 6 (2006) 662–668.
[79] W. Jiang, B.Y.S. Kim, J.T. Rutka, W.C.W. Chan, Nanoparticle-mediated cellular response is size-dependent, Nat. Nanotechnol. 3 (2008) 145–150.
[80] X.E. Jiang, C. Rocker, M. Hafner, S. Brandholt, R.M. Dorlich, G.U. Nienhaus, Endo- and exocytosis of Zwitterionic quantum dot nanoparticles by live HeLa cells, ACS Nano 4 (2010) 6787–6797.
[81] D. Banerjee, A.P. Liu, N.R. Voss, S.L. Schmid, M.G. Finn, Multivalent display and receptor-mediated endocytosis of transferrin on virus-like particles, Chembiochem 11 (2010) 1273–1279.
[82] H. Agrawal, M. Zelisko, L.P. Liu, P. Sharma, Rigid proteins and softening of biological membranes-with application to HIV-induced cell membrane softening, Sci. Rep. 6 (2016).
[83] C. Handel, B.U.S. Schmidt, J. Schiller, U. Dietrich, T. Mohn, T.R. Kiessling, S. Pawlizak, A.W. Fritsch, L.C. Horn, S. Briest, M. Hockel, M. Zink, J.A. Kas, Cell membrane softening in human breast and cervical cancer cells, New J. Phys. 17 (2015).
[84] C. Alibert, B. Goud, J.B. Manneville, Are cancer cells really softer than normal cells? Biol. Cell. 109 (2017) 167–189.
[85] C.Z. Zhang, Z.G. Wang, Nucleation of membrane adhesions, Phys. Rev. E (2008) 77.
[86] A. Salvati, A.S. Pitek, M.P. Monopoli, K. Prapainop, F.B. Bombelli, D.R. Hristov, P.M. Kelly, C. Aberg, E. Mahon, K.A. Dawson, Transferrin-functionalized nanoparticles lose their targeting capabilities when a biomolecule corona adsorbs on the surface, Nat. Nanotechnol. 8 (2013) 137–143.
[87] M.C. Lo Giudice, L.M. Herda, E. Polo, K.A. Dawson, In situ characterization of nanoparticle biomolecular interactions in complex biological media by flow cytometry, Nat. Commun. 7 (2016).
[88] S. Lara, F. Alnasser, E. Polo, D. Garry, M.C. Lo Giudice, D.R. Hristov, L. Rocks, A. Salvatit, Y. Yan, K.A. Dawson, Identification of receptor binding to the biomolecular corona of nanoparticles, ACS Nano 11 (2017) 1884–1893.